

# Highly Conducting and Stretchable Double-Network Hydrogel for Soft Bioelectronics

Gang Li, Kaixi Huang, Jue Deng, Mengxue Guo, Minkun Cai, Yuan Zhang, and Chuan Fei Guo\*

Conducting polymer hydrogels are promising materials in soft bioelectronics because of their tissue-like mechanical properties and the capability of electrical interaction with tissues. However, it is challenging to balance electrical conductivity and mechanical stretchability: pure conducting polymer hydrogels are highly conductive, but they are brittle; while incorporating the conducting network with a soft network to form a double network can improve the stretchability, its electrical conductivity significantly decreases. Here, the problem is addressed by concentrating a poorly crosslinked precursor hydrogel with a high content ratio of the conducting polymer to achieve a densified double-network hydrogel (5.5 wt% conducting polymer), exhibiting both high electrical conductivity ( $\approx 10 \text{ S cm}^{-1}$ ) and a large fracture strain ( $\approx 150\%$ ), in addition to high biocompatibility, tissue-like softness, low swelling ratio, and desired electrochemical properties for bioelectronics. A surface grafting method is further used to form an adhesive layer on the conducting hydrogel, enabling robust and rapid bonding on the tissues. Furthermore, the proposed hydrogel is applied to show high-quality physiological signal recording and reliable, low-voltage electrical stimulation based on an in vivo rat model. This method provides an ideal strategy for rapid and reliable tissue-device integration with high-quality electrical communications.

to exhibit tissue-like mechanical properties—soft, stretchable, and conformable to biotissues; and also needs to be highly conductive to enable high-quality electrical communications. Traditional bioelectronics are made of rigid materials like metals, which exhibit high electrical conductivity but large mechanical mismatch with biotissues, resulting in nonconformable electrode–tissue interface, and severe inflammation.<sup>[3]</sup> Soft bioelectronics were developed in recent years to replace the rigid components in traditional bioelectronics with tissue-like soft materials to improve the conformability and reduce the adverse immune responses,<sup>[4,5]</sup> and this area asks for high-performance soft conductors to realize the functionalities of such tissue-like bioelectronics.

Conducting polymer hydrogels are promising conductors that can serve as the electrodes for soft bioelectronics.<sup>[6,7]</sup> Hydrogels are water-rich networks that present high biocompatibility, tissue-like mechanical properties, and tunable functionalities desired for bioelectronics.<sup>[8,9]</sup>

However, it is a great challenge for a conducting polymer hydrogel to achieve both high conductivity and large stretchability.<sup>[8,10]</sup> Poly(3,4-ethylenedioxythiophene):polystyrene sulfonate (PEDOT:PSS) is the most promising conducting polymer. Pure PEDOT:PSS hydrogels have been reported to present a high conductivity on the level of  $\approx 40 \text{ S cm}^{-1}$ ,<sup>[11,12]</sup> but they are brittle because the single PEDOT:PSS network cannot effectively dissipate strain energy.<sup>[13]</sup> Incorporating the conducting polymer with another polymer network—by in situ polymerization of EDOT in an existing ductile network,<sup>[14,15]</sup> or by forming a second network in an existing PEDOT:PSS network to construct an interpenetrating polymer network (IPN),<sup>[16]</sup> can enhance the stretchability of the hydrogel, but a huge decrease in electrical conductivity ( $< 0.3 \text{ S cm}^{-1}$ ) is observed. Such a compromise between stretchability and conductivity is potentially attributed to the deteriorated continuity and the low content of the conductive network when an electrically insulated network is introduced,<sup>[8]</sup> or the limited solubility of commercially available PEDOT:PSS solution ( $\approx 1 \text{ wt}\%$ ).


Herein, we report a double-network (DN) conducting polymer hydrogel of PEDOT:PSS and poly(vinyl alcohol) (PVA) with high electrical conductivity ( $\approx 10 \text{ S cm}^{-1}$ ) and large stretchability

## 1. Introduction

The reliable integration of electronic devices with biotissues can enable electrical stimuli to biotissues and accurate biological signal recording, and has proven to be promising to treat diseases that are caused by the malfunction of bioelectronic system of the human body, such as the Parkinson's disease and heart arrhythmia.<sup>[1,2]</sup> A great challenge of the tissue-device integration lies in the difficulty to explore an ideal electrode: it needs

G. Li, K. Huang, J. Deng, M. Guo, M. Cai, Y. Zhang, C. F. Guo  
 Department of Materials Science and Engineering  
 Southern University of Science and Technology  
 Shenzhen 518055, China  
 E-mail: guocf@sustech.edu.cn

J. Deng  
 Department of Mechanical Engineering  
 Massachusetts Institute of Technology  
 Cambridge, MA 02139, USA

 The ORCID identification number(s) for the author(s) of this article can be found under <https://doi.org/10.1002/adma.202200261>.

DOI: 10.1002/adma.202200261

( $\approx 150\%$ ), by using an in situ aggregation and densification method that effectively increases the content of PEDOT:PSS in a DN network. Our strategy is to decrease the content of PVA to significantly enhance the relative mass ratio of PEDOT:PSS to PVA (to  $\approx 1:1$ ) in a precursor hydrogel, and then an acid treatment is used to build the highly conducting polymer networks and concentrate the solid components (PEDOT:PSS and PVA) by deswelling. A DN hydrogel with a high content of PEDOT:PSS ( $\approx 5.5$  wt%) is achieved, providing a high electrical conductivity of  $\approx 10$  S cm $^{-1}$  together with a large stretchability of 150%. In addition, the hydrogel exhibits excellent electrochemical properties (because the dense conducting network can restore more charges), tissue-like mechanical properties (excellent stretchability and low elastic modulus  $\approx 460$  kPa), high biocompatibility, and low swelling ratio (no detectable lateral swelling) in wet environment, making it suitable as implantable electrodes for bioelectronic applications. We further apply a surface grafting method to add an adhesive hydrogel on the stretchable conducting hydrogel for robust integration with tissues (high interfacial toughness over 200 J m $^{-2}$ ). We demonstrate that our electrical bioadhesive hydrogel can be adhered to muscles for stable and long-term in vivo electromyographic (EMG) signal recording in a rat model, and to a sciatic nerve for reliable electrical stimulation with a low stimulation voltage down to 125 mV. We expect that our electrode to be used in more applications in tissue-electronic interfaces, high-spatial-resolution neuromodulation, and other applications. Moreover, our method to make highly conductive and highly stretchable hydrogels might also be extended to other material systems to advance the development of next-generation bioelectronics.

## 2. Results and Discussion

### 2.1. Design and Fabrication of the Conductive Stretchable Hydrogels

We design a double-network hydrogel to achieve high stretchability and high electrical conductivity. In most stretchable and tough double-network hydrogels, one network is rigid and brittle, and the other is soft and ductile.<sup>[13]</sup> In our system, the PEDOT:PSS network is rigid and brittle; and we use the PVA network, which is loosely crosslinked, serving as the soft and stretchable one. We select PVA as the second network because the neutral PVA can mix with PEDOT:PSS without precipitation<sup>[17]</sup> and the crosslinking density of the PVA network can be well controlled.<sup>[18]</sup> The key point to improve the conductivity of the system is to enhance the content and uniformity of PEDOT:PSS in the double network. Commercially available PEDOT:PSS often has a low solubility in aqueous systems. Here, we provide a simple strategy to address the problem: At a maximum concentration of PEDOT:PSS, we minimize the content of PVA to achieve a high mass ratio of PEDOT:PSS to PVA in a precursor hydrogel; next, an acid treatment is used to significantly densify (or deswell) the precursor hydrogel to achieve a DN hydrogel with high PEDOT:PSS content and high uniformity (Figure 1a).

The preparation of the reagent solution is important to realize our design: the solution is prepared by adding 1.0 g PVA

power into 99 g PEDOT:PSS colloidal particle solution (Clevios PH 1000, solid content 1.0 wt%). This leads to a weight ratio of PEDOT:PSS to PVA of 1:1 in the solution, much higher than the ratio in existing PEDOT:PSS-based stretchable hydrogels.<sup>[19,20]</sup> All reagents involved in the preparation are shown in Figure 1b. Two steps are included to prepare the hydrogel. First, 100  $\mu$ L glutaraldehyde (GA) is added into the solution to crosslink PVA (Figures S1 and S2, Supporting Information). After gelation, the PEDOT:PSS colloidal particles are dispersed homogeneously in the PVA network without any precipitates (Figure S3, Supporting Information). We ascribe the homogeneous distribution of PEDOT:PSS in the PVA network to the low concentration of PVA and its neutral chains. This hydrogel (called “as-made hydrogel” hereinafter) is mechanically weak due to the low concentration of PVA (Figure S4, Supporting Information). Second, the as-made hydrogel is soaked in a large amount of pure acetic acid (HOAc). HOAc and PVA play an important role in converting PEDOT:PSS into a conducting network. HOAc replaces water in the as-made hydrogel. As a poor solvent for PVA and PEDOT:PSS, HOAc leads to the concentration of PVA and the aggregation of PEDOT:PSS, and the content of PVA and PEDOT:PSS increases profoundly from 2 to 40 wt%. Because the PEDOT:PSS colloidal particles are aggregated inside the PVA network, the dimension of the aggregates is locally constrained by the PVA network. Therefore, the PVA network serves as a template to constrain the aggregation of PEDOT:PSS into a continuous network. HOAc can also improve the electrical conductivity of the PEDOT:PSS network by increasing the ratio of PEDOT to PSS and inducing a more conducting configuration of PEDOT (Figure S5, Supporting Information).<sup>[21–23]</sup> The ratio between PEDOT and PSS is found to increase after the acid treatment because certain PSS is washed away during the soaking process, as evidenced in Figure S5a in the Supporting Information. The removal of the insulating PSS will improve the continuity of the PEDOT network and contribute to the high conductivity.<sup>[24]</sup> In addition, Raman spectrometry test in Figure S5b in the Supporting Information reflects the change in molecular structure of PEDOT. A red-shift in the acid-treated hydrogel is observed, suggesting that the PEDOT molecular structure transfers from benzoid to quinoid, which is a more conducting configuration.<sup>[24]</sup> The gel is finally soaked in deionized water to replace HOAc by water, forming a PEDOT:PSS/PVA DN hydrogel.

Note that the acid treatment causes no planar contraction of the hydrogel but only reduction in thickness; and the area of the specimen does not change when the acid-treated gel is soaked in water and transforms to the PEDOT:PSS/PVA DN hydrogel (Figure 1c). The anisotropic deswelling during the acid treatment is due to the modest interaction between the gel and the substrate (which is treated to be hydrophilic by oxygen plasma) that constrains the motion of the chains along the plane direction, while allowing the chains to rearrange in the thickness direction. By contrast, the as-made hydrogel significantly swells in water along both the plane direction and the thickness direction. The swelling ratios and corresponding solid contents (the weight ratio of PEDOT:PSS to PVA) of all these materials in reference to the as-made hydrogel are tested (Figure 1d). It shows that the acid-treated hydrogel has a densification factor of 5 (or a swelling ratio of 0.20) of the solids.

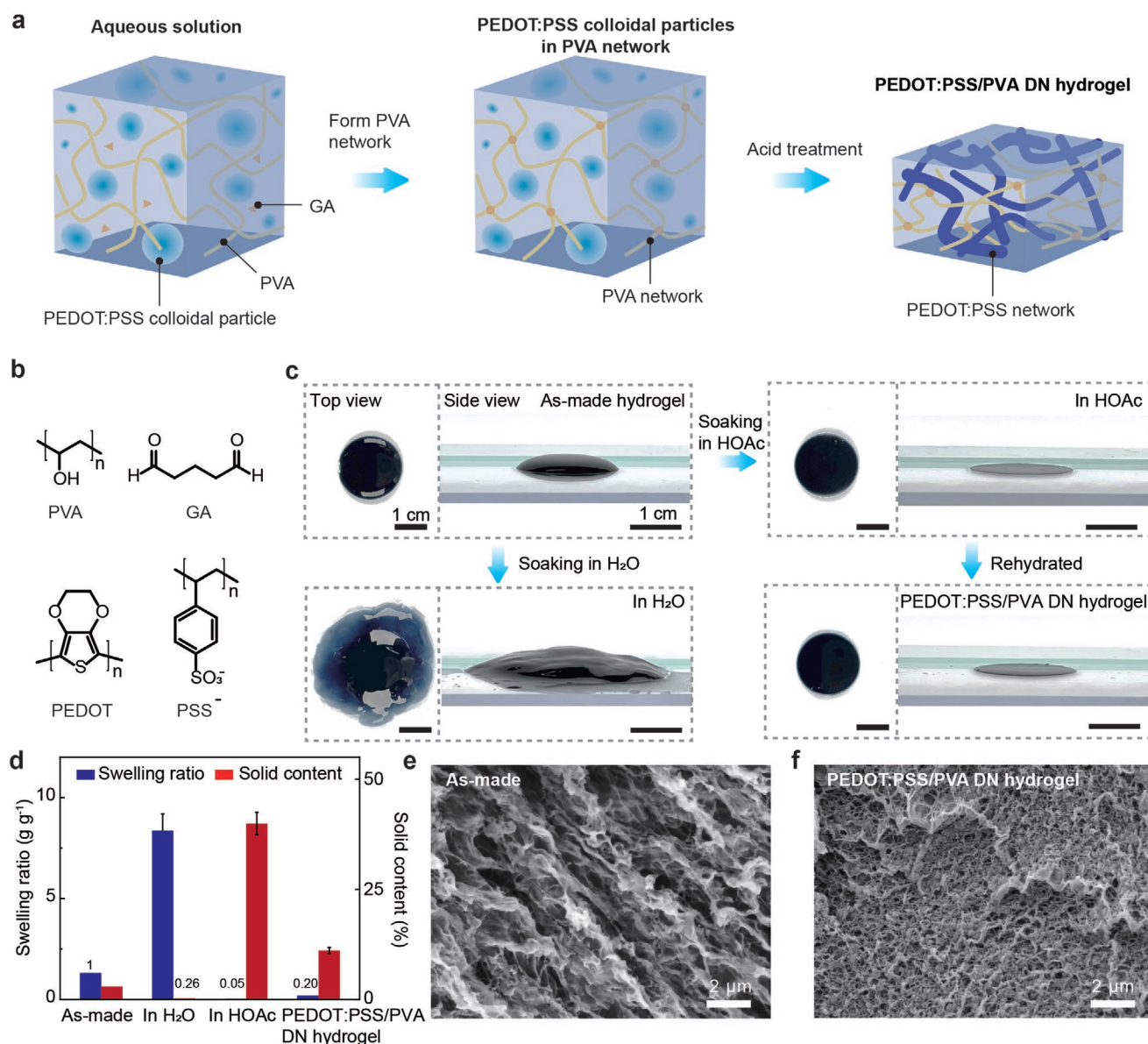


**Figure 1.** Fabrication of the PEDOT:PSS/PVA DN hydrogel. a) Schematic illustration of the fabrication and the structural change of PEDOT:PSS and PVA during the GA crosslinking and the acid treatment process. b) Reagents used for the fabrication. c) The swelling properties of the as-made hydrogel in water and in acetic acid, and that of the acid-treated hydrogel in water. d) Swelling ratio and solid content of the as-made hydrogel, as-made hydrogel swollen in water, as-made hydrogel treated by acid, and acid-treated gel swollen in water. e, f) Representative SEM images of the as-made (e) and PEDOT:PSS/PVA DN (f) hydrogels.

That is, the weight ratio of PEDOT:PSS (and also PVA) achieves  $\approx 5.5\%$ , which is much higher compared with the existing conducting IPN hydrogels. The densification of the hydrogel can be verified by our scanning electron microscopy (SEM) inspection over freeze-dried hydrogels. Figure 1e,f shows that the freeze-dried sample of the as-made hydrogel possesses large pores with an average diameter of 1–2  $\mu\text{m}$ . By contrast, the acid-treated sample shows a much denser network with small and uniform pores (an average diameter of  $\approx 100$  nm). The microstructure observation well explains the high electrical conductivity of the PEDOT:PSS/PVA hydrogel, and verifies the effectiveness of our method.

## 2.2. Mechanical and Electrical Properties of the Conductive and Stretchable Hydrogels

The densification makes the PEDOT:PSS/PVA hydrogel mechanically strong and stretchable. Figure 2a demonstrates that a hydrogel strip can be significantly elongated to  $\approx 100\%$  strain or significantly twisted and stretched without failure. In a uniaxial tension test, the hydrogel exhibits a large elongation (150%), and a low elastic modulus of 460 kPa (Figure 2b), which is on the same level of the rigidity of many biotissues such as muscles,<sup>[5]</sup> and five orders of magnitude lower than that of traditional metallic electrodes.<sup>[8]</sup> The large stretchability



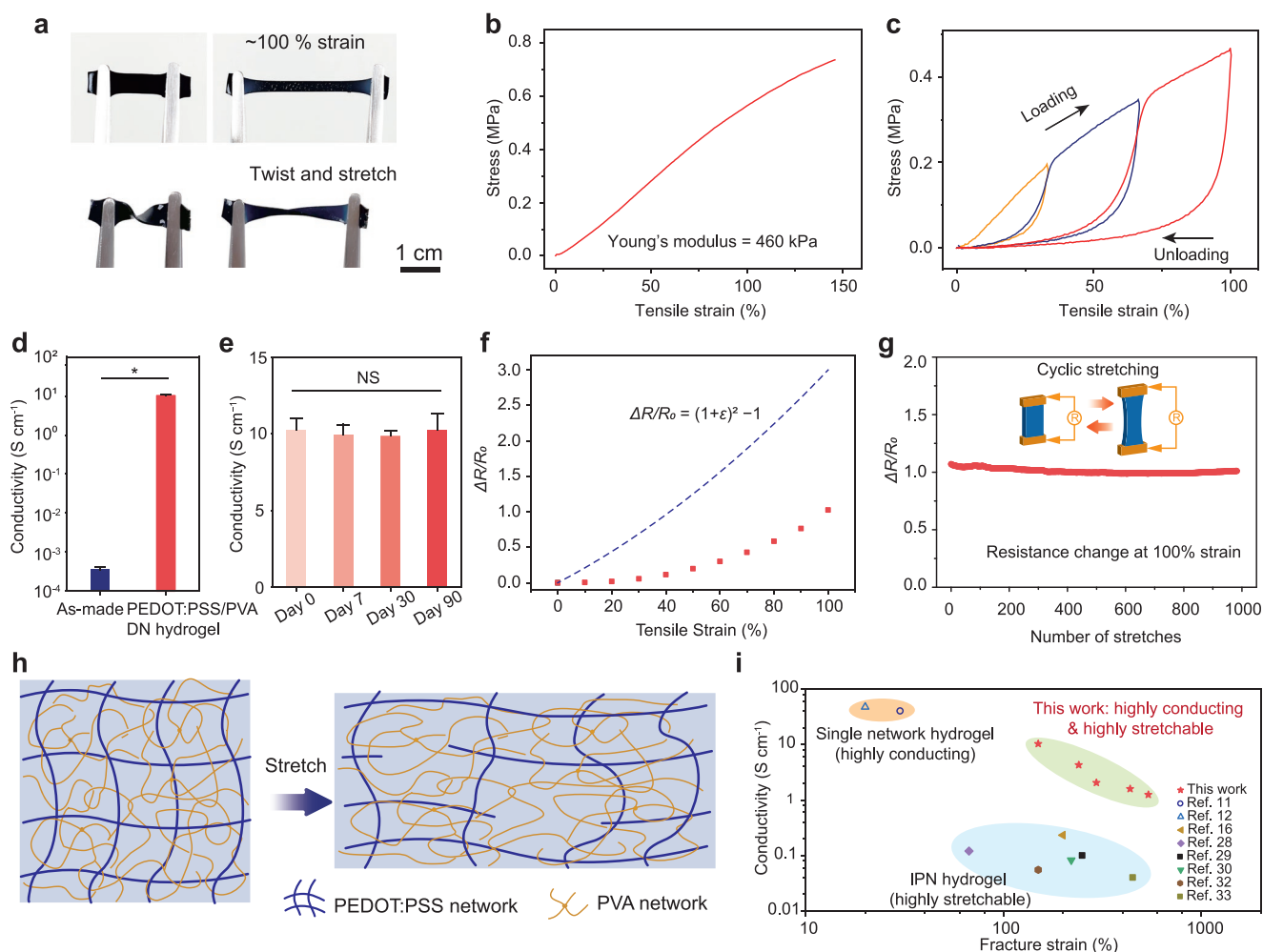


**Figure 2.** Mechanical and electrical properties of the PEDOT:PSS/PVA DN hydrogel. a) Representative photographs of the PEDOT:PSS/PVA DN hydrogel under stretching, twisting, and twisted stretching, showing that the hydrogel can survive at large strains. b) Stress-strain curve of the PEDOT:PSS/PVA DN hydrogel. c) Successive loading-unloading cycles of the PEDOT:PSS/PVA DN hydrogel. d) Electrical conductivity of the as-made hydrogel and the PEDOT:PSS/PVA DN hydrogel with acid treatment. e) Conductivity of the PEDOT:PSS/PVA DN hydrogel for 3 months, showing high stability overtime. f) Normalized change in resistance as a function of strain of the PEDOT:PSS/PVA DN hydrogel, and that for an ideal incompressible elastic conductor is present as a reference. g) Normalized change in resistance of the PEDOT:PSS/PVA DN hydrogel loaded to 100% strain over 1,000 cycles. h) Schematic illustration of the deformation mechanism of the PEDOT:PSS/PVA DN hydrogel. i) The comparison of the PEDOT:PSS/PVA DN hydrogel with single conducting polymer network and conducting polymer-based IPN hydrogels in terms of fracture strain and electrical conductivity. Our hydrogel presents combined high conductivity and high stretchability.

and tissue-like rigidity of the proposed hydrogel can meet the requirements of soft bioelectronics in the circumstances where large deformation is encountered. The successive loading cycles of the hydrogel reveal a large hysteresis in the first loading cycle, but this hysteresis cannot be observed in the next loading cycles (Figure 2c). This phenomenon is a result of the fracture of covalent bonds in the brittle conducting network (evidenced by the significant decrease in modulus in the subsequent cycles), which can be commonly observed in DN hydrogels.<sup>[13]</sup> In addition, similar to other DN hydrogels, the hydrogel becomes harder and less ductile when the crosslinking density of the PVA network increases (Figure S6, Supporting Information). These observations confirm the DN structure of the acid-treated PEDOT:PSS/PVA hydrogel.

The PEDOT:PSS/PVA DN hydrogel exhibits high electrical conductivity. The conductivity of the PEDOT:PSS/PVA DN

hydrogel reaches  $\approx 10 \text{ S cm}^{-1}$ , which is four orders of magnitude higher than that of the as-made hydrogel (Figure 2d). This value is comparable to the conductivity of single network PEDOT:PSS hydrogels (which have poor stretchability),<sup>[11,12,24,25]</sup> and 2–5 orders of magnitude higher than other stretchable PEDOT:PSS-based hydrogels.<sup>[19,20]</sup> At a thickness of 200  $\mu\text{m}$ , the sheet resistance of the PEDOT:PSS/PVA DN hydrogel is  $\approx 5 \text{ } \Omega$  per square, which is superior to that of commercial transparent electrodes of doped oxide films or metal meshes (10–400  $\Omega$  per square). The electrical and mechanical properties of the hydrogel are strongly related to the water content (Figure S7, Supporting Information). The electrical conductivity and Young's modulus increase with the decreasing of water content, while the stretchability decreases. In addition, the hydrogel maintains a stable electrical conductivity over 3 months in water (Figure 2e). The high conductivity and its high stability can ensure reliable

long-term applications of the hydrogel electrode in implantable bioelectronics.

The PEDOT:PSS/PVA DN hydrogel possesses robust electro-mechanical properties. Under tensile strains, the resistance of the hydrogel has a slow increase with strain. The normalized change in resistance ( $\Delta R/R_0$ ) of the hydrogel at 50% strain is only about 0.2, and increases to 1.1 when the hydrogel is stretched to 100% (Figure 2f). Note that the  $\Delta R/R_0$  value as a function of strain ( $\epsilon$ ) is even lower than that of ideal elastomeric conductors (such as ionic hydrogels), of which  $\Delta R/R_0 = (1 + \epsilon)^2 - 1$  is present, determined by the change in geometry of incompressible soft materials.<sup>[26]</sup> The slower increase in resistance of the hydrogel during stretching is related to its network structure. When the strain is small, the conductive network is stretched by molecular chain straightening, and little damage to the PEDOT chains occurs. As a result,  $\Delta R/R_0$  is only 0.02 at 20% strain, which is a negligible change. That is, the PEDOT:PSS/PVA DN hydrogel is strain insensitive, and its resistance can be considered to be unchanged at relatively low strains (<30% strain). This property is desired to enable highly stable electrical communications with dynamic tissues. As strain further increases, more chains are straightened and part of the straightened chains breaks, and thus the slope of the curve increases with strain. Note that straining will lead to a permanent damage to the conducting network: the resistance of the hydrogel is 1.5 times its initial value after it is fully released from 100% strain, and the stress-strain hysteresis cannot be recovered. However, the change in electrical conductivity is still limited. Specifically, little permanent change in resistance is introduced when the prestrain is lower than 50% (most tissues deform below this strain).

The high stretchability of the hydrogel can also be maintained over strain cycling. The  $\Delta R/R_0$  value of the hydrogel keeps almost unchanged ( $\Delta R/R_0 \approx 1.1$ ) when subjected to repeated stretches at 100% strain for 1000 cycles (Figure 2g). The cyclic stability of the PEDOT:PSS/PVA DN hydrogel can be explained by the structure of the double network (Figure 2h). In the first loading cycle, the PEDOT:PSS network partially breaks and forms a network with larger pocket sizes but such ruptures are delocalized, similar to the case in 2D metal nanomeshes.<sup>[27]</sup> This partially ruptured network is more stretchable, and it does not rupture further in the following stretches due to the significant energy dissipation of the double network.<sup>[13]</sup> As a result, the resistance of the hydrogel does not change over cycling. The high cyclic stability is critically important to ensure the functionality of implantable bioelectronics for which cyclic deformation is required. For example, in subcutaneous EMG signal recording, the muscle is under cyclic motion and it requires the electrode to perform stably under strain cycles.

### 2.3. Comparison with Other Conducting Polymer Hydrogels

The combined high electrical conductivity and high stretchability makes our PEDOT:PSS/PVA DN hydrogel superior among all conducting polymer hydrogels, and its comparison with existing conducting polymer hydrogels is shown in Figure 2i. For existing hydrogels, pure PEDOT:PSS hydrogels may present high conductivity on the order of  $10 \text{ S cm}^{-1}$ , but

they are weak and brittle.<sup>[11,12]</sup> Such hydrogel can survive only under small strains (less than 30%). Interpenetrating polymer networks are stretchable (stretchability can be larger than 100%), but their electrical conductivity values are much lower ( $0.001\text{--}0.23 \text{ S cm}^{-1}$ ).<sup>[28–33]</sup> Here, the electrical conductivity of our DN hydrogel with densified PEDOT:PSS is on the same order of magnitude with the pure PEDOT:PSS hydrogels, and can be cyclically stretched to 100% while showing limited decrease in electrical conductivity. With such a combined high electrical conductivity and high stretchability, our hydrogel is potentially useful as electrodes or interconnects to replace metal electrodes and hydrogel-based electrodes in muscle-like bioelectronics.

Our hydrogel also presents advantages in its fabrication. In traditional hybrid network hydrogels, the conducting polymer is in situ polymerized from monomers.<sup>[14,15]</sup> This method suffers from the problems of low solubility of monomers, low reaction conversion rate, poor homogeneity of the conducting network, and complicated procedure.<sup>[8]</sup> In this method, the two types of polymers are homogeneously interpenetrated with each other to form a densified DN hydrogel with highly conductive pathways. It presents several advantages: 1) nonbiocompatible small-molecule residual will not be introduced because of no polymerization in the fabrication. 2) The sample preparation is simple and highly reproducible. Low batch-to-batch repeatability generally leads to poor reliability in the applications due to the difficulties of in situ polymerization of PEDOT:PSS-based conducting polymer. 3) The properties of our hydrogel can be easily tuned by changing either the content of the crosslinker GA (Figure S6, Supporting Information) or the mass ratio between PEDOT:PSS and PVA. For example, the stretchability of the PEDOT:PSS/PVA DN hydrogel can be enhanced by increasing the content of PVA (Figure S8, Supporting Information). Starting from 95 wt% PEDOT:PSS solution and 5 wt% PVA, a hydrogel with 550% stretchability is obtained, while its electrical conductivity can still maintain a relatively high level of  $\approx 1 \text{ S cm}^{-1}$  (Figure S9, Supporting Information). For application scenarios where extremely large stretchability is required, our hydrogel is still competent.

### 2.4. Adhesive Performance and Electrochemical Properties

To increase the integrability and electrical reliability between implanted devices and biological tissues, we further introduce bioadhesive capability by simply grafting a tissue adhesive layer on the top of the PEDOT:PSS/PVA DN hydrogel (Figure 3a).<sup>[34,35]</sup> The PEDOT:PSS/PVA DN hydrogel is immersed in an aqueous solution of  $\alpha$ -ketoglutaric acid (KA) to absorb the photo-initiator in the bulk. A thin layer of the precursor of bioadhesive (35% acrylic acid (AAc), 3% acrylic acid *N*-hydroxysuccinimide ester (AAc-NHS), 7% PVA, 0.1% KA, and 0.05% poly(ethylene glycol) diacrylate (PEGDA) in water) is applied on the surface of hydrogel. After that, UV irradiation is applied to initiate the polymerization of the precursor to form a bioadhesive layer. The PEDOT:PSS/PVA DN hydrogel (water content  $\approx 89 \text{ wt\%}$ ) allows the monomers to diffuse in the bulk, which can polymerize with external AAc to form a network across the surface.<sup>[34]</sup> In this way, the bioadhesive layer is robustly integrated with the PEDOT:PSS/PVA DN hydrogel

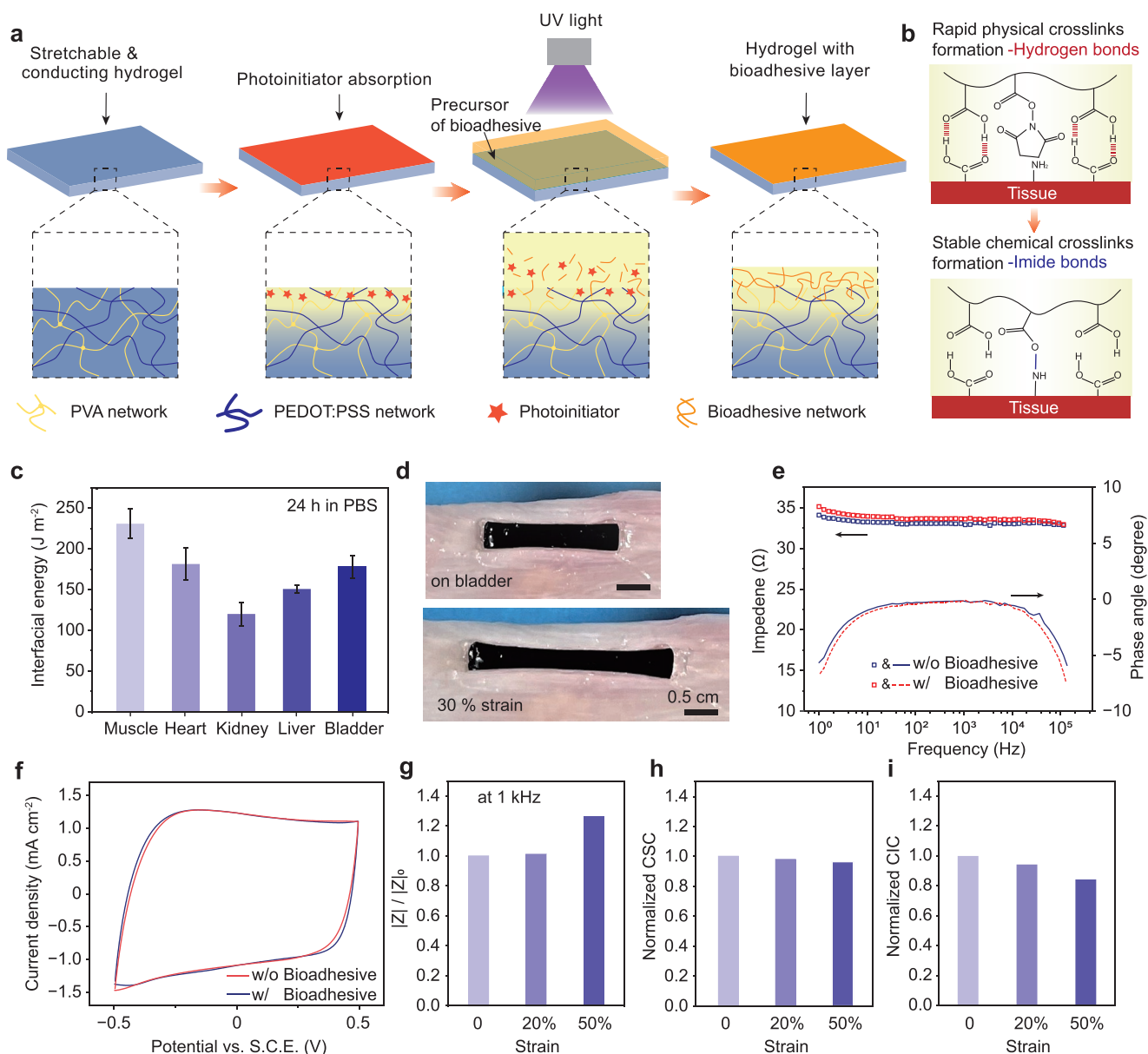


**Figure 3.** Adhesion property and electrochemical performance. a) Schematic illustration of the fabrication of adhesive layer on the PEDOT:PSS/PVA DN hydrogel. b) The physical interaction and covalent bonding between the bioadhesive and the tissue to form rapid and stable adhesion. c) Interfacial toughness of the conducting hydrogel electrode adhered after 24 h storage time. d) Photographs of the application of the conducting hydrogel electrode on bladder tissues, both at nonstrained and strained states. No delamination of the electrode is observed. e) Impedance and phase angle of the conducting stretchable hydrogel with and without an adhesive layer. f) Current density–voltage curves of the conductive stretchable hydrogel with and without an adhesive layer. g–i) Impedance, CSC, and charge injection capacity of the conducting stretchable hydrogel at different strains of 0%, 20%, and 50%, respectively.

(interfacial toughness  $\approx 600 \text{ J m}^{-2}$ , Figure S10, Supporting Information). The bioadhesive PEDOT:PSS/PVA hydrogel (which is termed as “conducting hydrogel electrode” hereinafter) is fully dried before use and adheres to tissue via a dry crosslinking mechanism.<sup>[36–38]</sup> In specific, once the adhesive side of the dried electrode is in contact with the tissue, the hydrophilic polymers (PAAc and PVA) of the bioadhesive absorb the interfacial water of the tissue and form rapid adhesion to the tissue via hydrogen bonding (Figure 3b and Figure S11, Supporting Information). Next, the NHS groups in the bioadhesive undergo a coupling

reaction with the primary amine group on the tissue surface within several minutes, creating covalent crosslinks. The bioadhesive PEDOT:PSS/PVA hydrogel can be applied to various tissues and maintain a high interfacial toughness value over 24 h in phosphate-buffered saline (PBS, pH 7.4), such as  $230 \pm 18 \text{ J m}^{-2}$  for muscle,  $181 \pm 20 \text{ J m}^{-2}$  for heart,  $120 \pm 14 \text{ J m}^{-2}$  for kidney,  $150 \pm 5 \text{ J m}^{-2}$  for liver, and  $178 \pm 14 \text{ J m}^{-2}$  for bladder (Figure 3c). The strong adhesion ensures the electrode to adhere on the tissue and conformably deform with the underlying tissues without any delamination after 24 h (Figure 3d).

Our hydrogel exhibits excellent electrochemical performance, and the grafted adhesive layer has little impact on the electrochemical performance. The conducting stretchable hydrogel samples (1 cm<sup>2</sup>) with and without an adhesive layer show similar impedance magnitudes (32.5–35.1  $\Omega$ ) and phase angles at the frequency range from 1 to 10 000 Hz (Figure 3e). The impedance values at low frequencies are lower than that of graphene-hydrogel composite.<sup>[37]</sup> In addition, both hydrogels with and without the adhesive layer exhibit similar cyclic voltammetry curves (Figure 3f). The charge storage capacity (CSC) is a key parameter for electrical stimulation. Our conducting hydrogel (200  $\mu\text{m}$  thick) with an adhesive layer exhibits a CSC of 48 mC cm<sup>-2</sup>, close to the reported value of pure PEDOT:PSS hydrogels (60 mC cm<sup>-2</sup>),<sup>[11]</sup> and much higher than that of Pt electrodes (0.55 mC cm<sup>-2</sup>)<sup>[39]</sup> and IrOx electrodes (28 mC cm<sup>-2</sup>).<sup>[40]</sup>

The stretchable and conducting hydrogel maintains high electrochemical performance under quasi-static and dynamic deformation. A PEDOT:PSS/PVA conducting hydrogel electrode adhered on pig tissue is incubated in PBS for 24 h before measuring the electrochemical properties. The impedance at the interface between adhered conducting hydrogel (1 cm<sup>2</sup>) and pig tissues increases with the increasing strains based on the electrochemical impedance spectroscopy measurement (Figure 3g). Specifically, the impedance at 1 kHz is 38.8  $\Omega$ , and slightly increases to 39.3 and 48.6  $\Omega$  at 20% and 50% strain, respectively. Furthermore, the overlapped current–voltage curves of the samples under different strains of 0%, 20%, and 50% indicate that strain has little impact on the CSC of our hydrogels (Figure 3h), potentially because that all PEDOT chains contribute to the charge storage under deformation. The charge injection capacity (CIC) is a critical parameter that evaluates electrical stimulation efficacy. The CIC value of the sample before loading is 250  $\mu\text{C cm}^{-2}$  (Figure S12, Supporting Information), and maintains 94.3% and 84.3% of the original value at the strain of 20% and 50%, respectively (Figure 3i). The high electrochemical performances of our conducting stretchable hydrogels under strained states may ensure stable signal recording and stimulating functionalities under body motion.

## 2.5. Cytotoxicity and Biocompatibility

The low cytotoxicity and high biocompatibility of bioelectronic materials are needed for prolonged application. We culture human umbilical vein endothelial cells (HUVECs) directly on top of the conducting hydrogel electrode to evaluate the cell viability and use the CCK-8 array to study the cytotoxicity of the hydrogel. The optical density (OD, which indicates the density of cells) values at 450 nm of the cell cultures with the conducting hydrogel electrode are compared with the regular wells at 24 and 72 h. No statistically significant differences in OD values for the two cases are observed (Figure 4a), suggesting the low cytotoxicity of the conducting hydrogel electrode. Furthermore, the in vivo biocompatibility of the conducting hydrogel electrode is studied by the subcutaneous implantation for 14 days. A conducting hydrogel electrode is implanted on the biceps femoris of a rat. After 14 days of implantation, histological assessments present minimal inflammatory response

(Figure 4b,c). In addition, the average inflammation thickness of the tissue adhered with the conducting hydrogel electrode is 135  $\mu\text{m}$ , which is close to that of the traditional Au electrode.<sup>[37]</sup>

## 2.6. In Vivo Electrical Signal Recording and Neural Stimulation

The electrical, mechanical, and biocompatible properties of the conducting hydrogel electrode enable potential applications for bioelectrical communications between electronics and biological tissues. As a proof of concept, we demonstrate the recording of EMG signals and sciatic neural stimulation based on a rat model. Two PEDOT:PSS/PVA conducting hydrogel electrodes are completely implanted on the right biceps femoris (which is one of the most dynamic tissues) of a rat with two leading wires connected to a head connector for chronic EMG recording (Figure 4d). The implanted conducting hydrogel electrodes show robust adhesion without any delamination or lateral swelling even when we squeeze the electrodes using tweezers (Figure 4e). Figure 4f,g shows the recorded EMG signals of a running rat at day 7 and day 14 after implantation. It shows that the EMG signals from different durations of implantation are close in both signal and noise magnitude levels, indicating that the electrode properties and the tissue–electrode interfaces are all stable during long-term implantation. Compared with other EMG electrodes (Table S1, Supporting Information), our electrode is soft, biocompatible, and stable in physiological environment, providing an excellent selection as implantable EMG electrodes for long-term signal recording. Our electrode can adhere to wet tissues via dry-crosslinking, enabling reliable integration with tissues to avoid unstable electrical communication during the implantation.

Further, our hydrogel electrodes are used for neural stimulation. Two electrodes are laminated on the surface of a sciatic nerve and strong adhesion of the electrode–tissue interface is achieved (Figure 4h,i). Rectangular voltage pulses with a 25 ms duration is applied and the ankle joint movement angle of the leg is recorded to assess the stimulation performance. Leg movements start to occur at a low voltage of 125 mV; and the movement angle increases to 18° as the voltage increases to 150 mV, and further increases to 22° at 300 mV (Figure 4j–l). The working voltages are much lower than that of the graphene-hydrogel composite (750 mV).<sup>[37]</sup> We ascribe the low stimulation voltage to the low impedance and high CIC of the PEDOT:PSS/PVA DN hydrogel. We expect the conducting hydrogel electrode to be further applied in neuromodulation, which can reduce the risk of damaging neural tissues.

## 3. Conclusions and Outlook

We have developed an in situ aggregation and densification method to achieve a stretchable and conducting hydrogel electrode with high conductivity of 10 S cm<sup>-1</sup> and a high stretchability of 150% simultaneously, overcoming the dilemma of stretchability and electrical conductivity in the existing conducting hydrogels. With stable electrochemical performance under deformation, low cytotoxicity, and high biocompatibility, the proposed conducting hydrogel electrodes are integrated



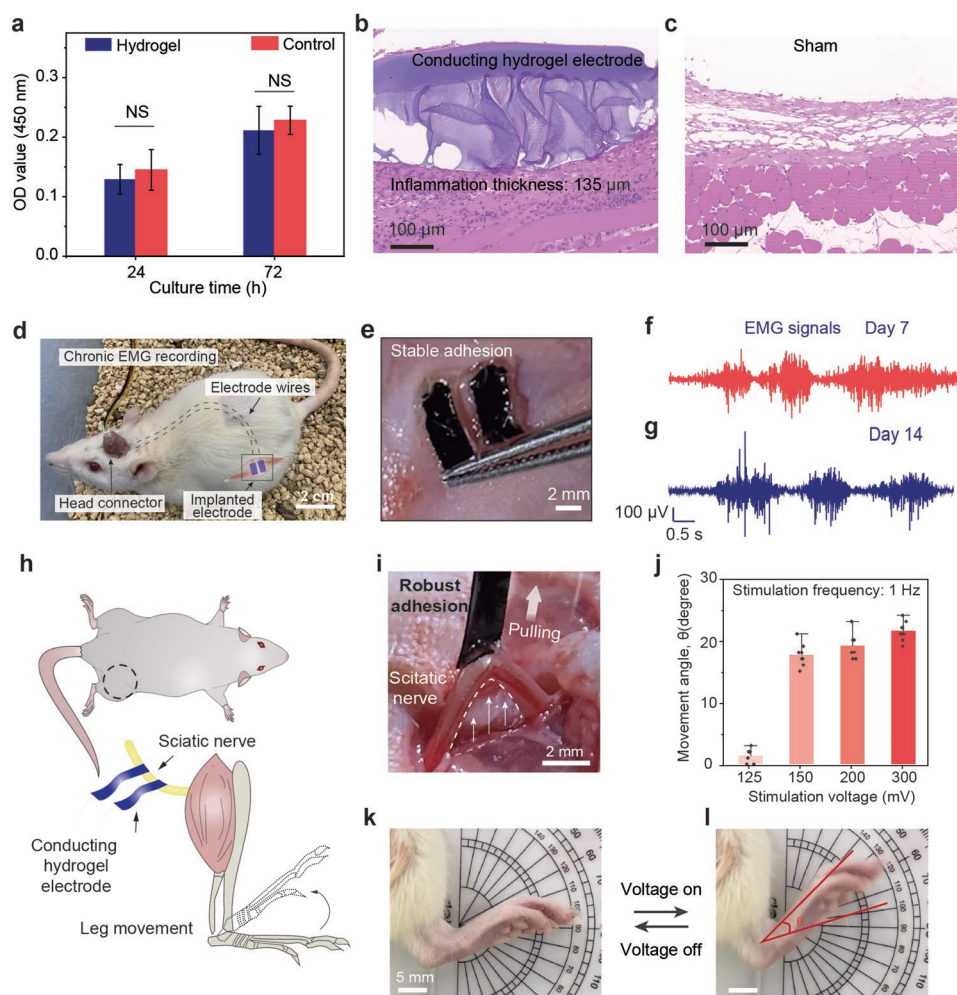


**Figure 4.** Cytotoxicity and biocompatibility of the conducting hydrogel electrode and its applications in implantable bioelectronics. a) Optical densities of a regular well and the well using our hydrogel electrode as the substrate for cell culture. No significant difference in optical density was observed for the two wells. b,c) Representative histological images of the hydrogel–tissue interface (b) and the control sample without conducting hydrogel electrode (c) stained with hematoxylin and eosin, showing a small inflammation thickness of 135  $\mu\text{m}$ . d) Photograph of a rat for chronic EMG recording. e) Photograph of two conducting hydrogel electrodes adhered on muscle for EMG recording. f,g) EMG signals recorded using the conducting hydrogel electrodes after 7 days (f) and 14 days (g) implantation. h) Schematic illustration of neural stimulation on rat using the conducting hydrogel electrode. i) Photograph showing robust integration of the conducting hydrogel electrode with a sciatic nerve. j) Movement angle of the rat leg under different stimulation voltages. k,l) Photographs showing the motion of the leg when the stimulation is off and on.

with the rat biceps femoris for chronic EMG recording and sciatic nerve for electrical stimulation, demonstrating the reliable bioelectronic functionalities in the deformable physiological conditions.

The high stretchability and high conductivity of the hydrogel may further enable high-resolution micro-bioelectronics. Metal-based electrode arrays can be minimized, but they suffer from the mechanical mismatch and chronic performance deterioration; existing stretchable hydrogels can match the mechanical properties of tissues, but they may not provide sufficient electrical conductivity to collect high signal-to-noise electrophysiological signals when the electrode pixels are reduced to a sub-millimeter scale. Our hydrogels are highly conducting, and can provide adequate signal-to-noise ratio when the material is significantly minimized. Ideally, the size of the minimized electrodes of our hydrogel can be reduced to at least

100 times smaller than existing stretchable hydrogels, since its conductivity is two orders of magnitude higher.<sup>[16]</sup> Overall, we envision that the stretchable and conducting hydrogel in this study may not only provide a strategy for reliable electrical communications with deformable biological tissues, but also contribute toward the development of next-generation stretchable bioelectronics.

## 4. Experimental Section

**Materials:** PEDOT:PSS colloidal solution Clevios PH 1000 was purchased from commercial sources. PVA ( $M_w$  146 000–186 000), GA (25% in  $\text{H}_2\text{O}$ ), acetic acid (>99%), AAc, PEGDA ( $M_n$  575), KA, and AAc-NHS were brought from Sigma-Aldrich. All reagents were used as received.



**Preparation of the PEDOT:PSS/PVA DN Hydrogel:** 1 g of PVA powders and 99 g PH 1000 solution were added into a 250 mL round bottom flask. The PVA was dissolved after heating at 90 °C for 1 h. The obtained solution was cooled down to room temperature and filtered through a poly(tetrafluoroethylene) (PTFE) membrane (pore dimension 0.8  $\mu\text{m}$ ). Next, 100  $\mu\text{L}$  GA solution was added into the PH 1000/PVA solution. A planetary mixer (Thinky ARE-310) was used to mix the GA in the polymer solution. After that, the precursor solution was transferred to a piece of PVC sheet and allowed to react for 6 h. During the reaction, a plastic lid was covered on the sheet to prevent water evaporation. Acid treatment was performed by immersing the GA crosslinked hydrogel (termed as as-made hydrogel) in acetic acid for 6 h followed by a throughout rinse in water to form the PEDOT:PSS/PVA DN hydrogel. PEDOT:PSS/PVA DN hydrogels with higher PVA contents were prepared in the similar procedure by simply changing the weight ratio of PH 1000 and PVA in the starting mixture.

**Preparation of the Adhesive Layer:** Two solutions were prepared for the surface grafting treatment. The first solution was a KA solution which was formed by dissolving 10 wt% KA in water. The second solution was a AAc-PVA solution which was prepared by dissolving 35 wt% AAc, 7 wt% PVA, 3 wt% AAc-NHS, 0.1 wt% KA, and 0.05 wt% PEGDA in water. The PEDOT:PSS/PVA hydrogel was soaked in the KA solution for 10 min and rinsed by water. Then the sample was placed on a glass, and the AAc-PVA solution was coated on top of the sample. Another glass was covered on the solution. The thickness of the solution was controlled by using spacers. The grafting layer was formed by UV-radiation for 30 min (284 nm, 10 W power). The formed bioadhesive hydrogel was dried in nitrogen and sealed in a plastic bag with desiccant and stored at  $-20\text{ }^{\circ}\text{C}$  for use.

**Characterization of the As-Made Hydrogel:** After mixed solution of PH 1000, PVA, and GA was loaded in the gap of rheometer (TA RS-2, 40 mm parallel plates) immediately. A layer of thin silicon oil was used to seal the mixture. Time-sweep test by measuring  $G'$  and  $G''$  at a shear strain of 1% and an oscillation frequency of 10  $\text{rad s}^{-1}$  was applied to monitor the reaction for a period of 10 h. After the time sweep test, the viscoelastic property of the gel was measured at a shear strain of 1% and a frequency range from 0.1 to 100  $\text{rad s}^{-1}$ .

**Tension Test of the PEDOT:PSS/PVA DN Hydrogel:** The PEDOT:PSS/PVA DN hydrogels were cut into a dog-bone shape (35 mm in length, 12 mm in gauge length, 2 mm width) and the tensile properties were measured in a universal testing machine (XLD-100E, Jingkong Mechanical testing Co., Ltd.) at a constant tensile speed of 100  $\text{mm min}^{-1}$ .

**Electrical Conductivity Characterization:** The electrical conductivity was calculated by taking the reciprocal of resistivity, which was equaled to the sheet resistance (measured by four-point method, Keithley 4200) divided by the thickness (measured by Microscope, Leica DM2700M). The electrical conductivity under strain was measured by stretching the sample using a home-made machine at a rate of 1  $\text{mm s}^{-1}$  and recording the two ends resistance using a digital multimeter (Keithley 2100).

**Electrochemical Property Test:** A strip of hydrogel with an area of 1  $\text{cm}^2$  was first fully dried. One end of the dried film was connected to silver wire using silver paste. The joint was further protected using a thin layer of silicon glue (Silpoxy, Smooth-on). The sample was immersed in PBS for adequately long time before test. The electrochemical properties were measured in PBS solution in a three electrodes setup with an electrochemical workstation (CS series, Wuhan CorrTest Instruments Corp., Ltd.), where the PEDOT:PSS/PVA DN hydrogel served as the working electrode, a Pt plate (1  $\text{cm}^2$ ) served as the counter electrode, and a saturated calomel electrode (S.C.E.) served as the reference electrode. Impedance was measured in the range from 10 kHz to 1 Hz. The CSC was measured by cyclic voltammetry (in the range of  $-0.5$  to  $0.5\text{ V}$ , scan rate 20  $\text{mV s}^{-1}$ ) and calculated by integrating the cathodic current with time (the curve of the third cycle was used).

**Adhesion Test:** All samples were pressed on various tissues (with  $\approx 1\text{ kPa}$  pressure for 5 s) and tested after 24 h to ensure the equilibrium swelling state. The interfacial toughness was measured using the 180° peel test with a universal testing machine (XLD-100E, Jingkong

Mechanical testing Co., Ltd.) at a constant peeling speed of 50  $\text{mm min}^{-1}$  and determined as the plateau force by the width of the hydrogel samples.

**Cytotoxicity and Biocompatibility:** The cell cytotoxicity of conducting hydrogel electrode was measured with HUVECs using the CCK-8 assay kit. The sterilized hydrogel disks (9 mm in diameter) were placed into a clear 48-well cell plate. HUVECs were seeded on the hydrogel disks at a density of  $1.0 \times 10^4$  cells per well, and incubated in 5%  $\text{CO}_2$  humidified atmosphere at 37 °C. After incubation for 24 and 72 h, 10  $\mu\text{L}$  of CCK-8 was added into each well, followed by incubation for another 2 h at 37 °C. The optical density at 450 nm was then measured using a Cytation 1 Cell Imaging Multi-Mode Reader (BioTek Instrument, USA). Growth medium without sample was used as control.

The bioadhesive conducting hydrogel electrodes were prepared in an aseptic manner and were disinfected under UV light for 3 h. Animals were anesthetized using isoflurane (2% in oxygen) in an anesthetizing chamber. Anesthesia was maintained using a nose cone (1.5% in oxygen). The back hair of the animals was removed and the subcutaneous space was accessed by skin incision. The subcutaneous space was created by blunt dissection. The samples were put into the subcutaneous pocket. The incision was sutured by 4-0 PGA wire (Jinhuan). The animals were killed by  $\text{CO}_2$  inhalation after 14 days of the implantation. The subcutaneous regions of interest were excised and fixed in 10% formalin for 24 h for histological analyses. Fixed tissue samples were placed in 70% ethanol. The tissue samples were then subjected to histological processing, followed by hematoxylin and eosin staining at Wuhan Servicebio Technology Co., Ltd.

**In Vivo Electromyographic Measurement:** The dried bioadhesive conducting hydrogel electrode was connected to PTFE-coated silver wires (AWG-40) using silver paste. The joint was further protected by Silpoxy glue. All samples were prepared in an aseptic manner and were further disinfected under UV light for 3 h.

The animals were anesthetized (1–3% isoflurane in oxygen). Three skin incisions were created. The first skin incision was on the leg of a rat to implant two electrodes on the biceps femoris. The second one was on the head to fix a head connector. Two holes were drilled on the skull using a microdrill (78001, RWD) and two screws were screwed in the skull. The head connector was placed on the screws and the fixation was done by curing bone cement between the plastic connector and the screws. The third incision was on the back, where the wires from the electrodes were connected to the wire from the head connector. The wires were threaded through the subcutaneous space which was created by blunt dissection. The incisions were then closed by sutures. Animals were allowed to recover for 1 week before EMG test. EMG signal was measured by connecting the head connector to a micro-4 system (Cambridge Electronic Design Limited) and recording when the animal was moving freely in the cage.

**In Vivo Sciatic Nerve Stimulation:** The bioadhesive conducting hydrogel electrodes were cut to 1.5 mm in width and 30 mm in length, and connected to a silver wire using silver paste. All samples were prepared in an aseptic manner and were further disinfected under UV light for 3 h.

The animals were anesthetized (1–3% isoflurane in oxygen). Skin incision was created on the thigh after shaving. The sciatic nerve was exposed by dissecting the vastus lateralis muscle and biceps femoris muscle. The bioadhesive conducting hydrogels were adhered on the exposed sciatic nerve. Biphasic charge-balanced rectangular voltage pulses (1 Hz, 0.10–0.3 V) were applied using an isolated stimulator (DS2A, Digitimer). The angle of the ankle joint was measured using a protractor marker placed under the leg.

**Animal Experiment Protocols:** All animal tests were compliant with the standard guidelines approved by the Southern University of Science and Technology (SUSTech) Ethics Committee, and all animal surgeries were reviewed and approved by the Committee on Animal Care at SUSTech (SUSTech-JY202012007, SUSTech-JY202110002, and SUSTech-JY202112010).

**Statistical Analysis:** The statistical significance of the comparison studies was evaluated by MATLAB (ver. R2020a). Data distribution was assumed to be normal for all parametric tests, but this was not formally tested. In the statistical analysis for comparison between

multiple samples, one-way analysis of variance (ANOVA) followed by Tukey's multiple comparison test was conducted with thresholds of  $*p \leq 0.05$ . For the statistical analysis between two data groups, a two-sample Student's *t*-test was used, and the significance thresholds were  $*p \leq 0.05$ .

## Supporting Information

Supporting Information is available from the Wiley Online Library or from the author.

## Acknowledgements

G.L., K.H., and J.D. contributed equally to this work. The work was funded by the National Natural Science Foundation of China (no. 52073138), the "Guangdong Innovative and Entrepreneurial Research Team Program" under Contract no. 2016ZT06G587, the "Science Technology and Innovation Committee of Shenzhen Municipality" (grant no. JCYJ20210324120202007), the Shenzhen Sci-Tech Fund (no. KYTDPT20181011104007), and the financial support from SUSTech-MIT MechE joint center. The authors thank Prof. Fuzeng Ren and Dr. Ju Fang for their help in cell cytotoxicity experiment. The authors also acknowledge the technical support from the SUSTech Core Research Facilities and the SUSTech Laboratory Animal Research Center, especially to Hui Guo for her help during the animal experiments.

## Conflict of Interest

The authors declare no conflict of interest.

## Data Availability Statement

The data that support the findings of this study are available from the corresponding author upon reasonable request.

## Keywords

conducting polymers, double-network hydrogels, electrode-tissue integration, in situ aggregation, PEDOT:PSS

Received: January 10, 2022

Revised: January 27, 2022

Published online: March 7, 2022

- [1] M. L. Kringelbach, N. Jenkinson, S. L. Owen, T. Z. Aziz, *Nat. Rev. Neurosci.* **2007**, *8*, 623.
- [2] H. Ouyang, Z. Liu, N. Li, B. Shi, Y. Zou, F. Xie, Y. Ma, Z. Li, H. Li, Q. Zheng, *Nat. Commun.* **2019**, *10*, 1821.
- [3] S. P. Lacour, G. Courtine, J. Guck, *Nat. Rev. Mater.* **2016**, *1*, 16063.
- [4] G. Schiavone, S. P. Lacour, *Sci. Transl. Med.* **2019**, *11*, eaaw5858.
- [5] R. Feiner, T. Dvir, *Nat. Rev. Mater.* **2017**, *3*, 17076.
- [6] L. V. Kayser, D. J. Lipomi, *Adv. Mater.* **2019**, *31*, 1806133.
- [7] Y. Liu, V. R. Feig, Z. Bao, *Adv. Healthcare Mater.* **2021**, *10*, 2001916.
- [8] H. Yuk, B. Lu, X. Zhao, *Chem. Soc. Rev.* **2019**, *48*, 1642.
- [9] X. Liu, J. Liu, S. Lin, X. Zhao, *Mater. Today* **2020**, *36*, 102.
- [10] Q. Peng, J. Chen, T. Wang, X. Peng, J. Liu, X. Wang, J. Wang, H. Zeng, *InfoMat* **2020**, *2*, 843.
- [11] B. Lu, H. Yuk, S. Lin, N. Jian, K. Qu, J. Xu, X. Zhao, *Nat. Commun.* **2019**, *10*, 1043.
- [12] Y. Liu, J. Liu, S. Chen, T. Lei, Y. Kim, S. Niu, H. Wang, X. Wang, A. M. Foudeh, J. B.-H. Tok, Z. Bao, *Nat. Biomed. Eng.* **2019**, *3*, 58.
- [13] J. P. Gong, *Soft Matter* **2010**, *6*, 2583.
- [14] T. Dai, X. Qing, Y. Lu, Y. Xia, *Polymer* **2009**, *50*, 5236.
- [15] T. Dai, X. Qing, H. Zhou, C. Shen, J. Wang, Y. Lu, *Synth. Met.* **2010**, *160*, 791.
- [16] V. R. Feig, H. Tran, M. Lee, Z. Bao, *Nat. Commun.* **2018**, *9*, 2740.
- [17] P. Li, K. Sun, J. Ouyang, *ACS Appl. Mater. Interfaces* **2015**, *7*, 18415.
- [18] H. S. Mansur, C. M. Sadahira, A. N. Souza, A. A. P. Mansur, *Mater. Sci. Eng., C* **2008**, *28*, 539.
- [19] Q. Liu, J. Qiu, C. Yang, L. Zang, G. Zhang, E. Sakai, *Adv. Mater. Technol.* **2021**, *6*, 2000919.
- [20] Y.-F. Zhang, M.-M. Guo, Y. Zhang, C. Y. Tang, C. Jiang, Y. Dong, W.-C. Law, F.-P. Du, *Polym. Test.* **2020**, *81*, 106213.
- [21] J. Y. Ouyang, *ACS Appl. Mater. Interfaces* **2013**, *5*, 13082.
- [22] Y. Xia, J. Ouyang, *ACS Appl. Mater. Interfaces* **2010**, *2*, 474.
- [23] H. Shi, C. Liu, Q. Jiang, J. Xu, *Adv. Electron. Mater.* **2015**, *1*, 1500017.
- [24] B. Yao, H. Wang, Q. Zhou, M. Wu, M. Zhang, C. Li, G. Shi, *Adv. Mater.* **2017**, *29*, 1700974.
- [25] S. Zhang, Y. Chen, H. Liu, Z. Wang, H. Ling, C. Wang, J. Ni, B. Çelebi-Saltik, X. Wang, X. Meng, *Adv. Mater.* **2020**, *32*, 1904752.
- [26] C. Keplinger, J.-Y. Sun, C. C. Foo, P. Rothmund, G. M. Whitesides, Z. Suo, *Science* **2013**, *341*, 984.
- [27] C. F. Guo, T. Sun, Q. Liu, Z. Suo, Z. Ren, *Nat. Commun.* **2014**, *5*, 3121.
- [28] Y. Shi, M. Wang, C. Ma, Y. Wang, X. Li, G. Yu, *Nano Lett.* **2015**, *15*, 6276.
- [29] W. W. Li, F. X. Gao, X. Q. Wang, N. Zhang, M. M. Ma, *Angew. Chem., Int. Ed.* **2016**, *55*, 9196.
- [30] Z. W. Wang, J. Chen, Y. Gong, H. Zhang, T. Xu, L. Nie, J. Fu, *Chem. Mater.* **2018**, *30*, 8062.
- [31] J. Hur, K. Im, S. W. Kim, J. Kim, D. Y. Chung, T. H. Kim, K. H. Jo, J. H. Hahn, Z. A. Bao, S. Hwang, N. Park, *ACS Nano* **2014**, *8*, 10066.
- [32] Y. Zhao, B. Zhang, B. Yao, Y. Qiu, Z. Peng, Y. Zhang, Y. Alsaid, I. Frenkel, K. Youssef, Q. Pei, X. He, *Matter* **2020**, *3*, 1196.
- [33] Y. Peng, B. Yan, Y. Li, J. Lan, L. Shi, R. Ran, *J. Mater. Sci.* **2020**, *55*, 1280.
- [34] H. Yuk, T. Zhang, G. A. Parada, X. Liu, X. Zhao, *Nat. Commun.* **2016**, *7*, 12028.
- [35] G. Li, Z. Qiu, Y. Wang, Y. Hong, Y. Wan, J. Zhang, J. Yang, Z. Wu, W. Hong, C. F. Guo, *ACS Appl. Mater. Interfaces* **2019**, *11*, 10373.
- [36] H. Yuk, C. E. Varela, C. S. Nabzdyk, X. Mao, R. F. Padera, E. T. Roche, X. Zhao, *Nature* **2019**, *575*, 169.
- [37] J. Deng, H. Yuk, J. Wu, C. E. Varela, X. Chen, E. T. Roche, C. F. Guo, X. Zhao, *Nat. Mater.* **2021**, *20*, 229.
- [38] S. J. Wu, H. Yuk, J. Wu, C. S. Nabzdyk, X. Zhao, *Adv. Mater.* **2021**, *33*, 2007667.
- [39] T. Rose, L. Robblee, *IEEE Trans. Biomed. Eng.* **1990**, *37*, 1118.
- [40] S. J. Wilks, S. M. Richardson-Burn, J. L. Hendricks, D. Martin, K. J. Otto, *Front. Neuroeng.* **2009**, *2*, 7.